EVALUATION STUDY OF COMPOSITE REINFORCED WING PANEL CONSTRUCTION

J.J. Cools and G. Bartelds
Fokker-VFW, Manufacturing Research and Production Development Department,
Schiphol, The Netherlands and
National Aerospace Laboratory NLR, Structures Department,
Amsterdam, The Netherlands

ABSTRACT

The application of HTS carbon-epoxy composite material in hybrid laminates and as reinforcement to aluminium wing panel construction is studied. Basic properties and compressive buckling behaviour of aluminium/carbon-epoxy hybrid laminates are determined using flat plate strips, folded short column sections and hat-stiffened panel specimens. It appears that a 30 percent weight saving as compared to all-metal short column can be achieved. It has not yet been fully evaluated what portion of this saving can be preserved in actual compression panel construction but 20 percent appears to be feasible. The application of composite reinforcement to improve fail-safe characteristics of stiffened and sandwich panels is shown to be very promising also. Although crack growth rates in aluminium parts are adversely affected by tensile pre-stress the crack arrest and residual strength characteristics are improved very significantly.

1. INTRODUCTION

In the Netherlands, the investigations into the applicability of composite materials in aerospace structures are carried out in joint programs by the aircraft company Fokker-VFW, the National Aerospace Laboratory NLR and the Aerospace Department of the University of Technology in Delft. The investigations are mainly concentrated on HTS-carbon fibres in an epoxy matrix, as this type of composite material is considered to offer the best possibilities for economical applications in commercial aircraft. Not only all-ca/ep-laminates, but also hybrids of ca/ep with other types of low cost fibre composites or sheet metal are being studied for use in stiffened skin and sandwich structures.

Working groups have been formed which are in charge of the next main areas of investigation:
(a) experimental determination of the mechanical, physical and chemical properties of the composite material(s),
(b) theoretical and experimental studies to obtain basic design data and procedures for designing optimum structures,
(c) development of non-destructive testing and inspection methods,
(d) application studies to obtain design and manufacturing experience by designing, building and testing secondary aircraft components.

In this paper, only the results of those theoretical and experimental programs are presented, which are aimed at the design of stiffened skin panels of which the skins and stringers consist of hybrid laminates and of selective reinforcement of metal structures.

2. HYBRID LAMINATES

2.1 General description

In the hybrid laminate concept developed at Fokker-VFW the composite material is sandwiched between two relatively thin metallic faces. In the case of a uni-directional composite core the hybrid laminate shows the following features
- the composite core is used to its full load carrying capacity
- the low transverse and shear stiffness properties of the core are compensated for by the metallic faces
- the metallic outer layers provide electrical conductivity and also protection against rain and sand erosion, moisture absorption and oxidation
- the thermal stresses generated due to thermal incompatibility of the constituent materials must be considered as an unfavourable aspect.

2.2 Compression panel development

This program is aimed at the development of calculation methods to predict the strength of stiffened skin panels made out of orthotropic hybrid laminates. It started out with the investigation of flat plates, then continued with short column sections and was provisionally concluded with skin-stringers panels.

2.2.1 Flat plates

The available information from the literature limited a theoretical analysis of compression loaded flat orthotropic plates to the initial, critical buckling strength. No data were found for the calculation of the ultimate buckling strength.

The elastic, critical buckling load per unit width of an infinitely long flat orthotropic plate, simply supported along the four edges, is given by:

$$p_x = \frac{\pi^2}{b^2}\left[2\sqrt{D_x D_y} + \nu_{yx} D_y + \nu_{xy} D_x + 4 D_{xy}\right] \quad (1)$$

where b is the width of the strip and the stiffness quantities D are defined as

$$D_x = \int_{\text{thickness}} \frac{E_x z^2 dz}{1-\nu_{xy}\nu_{yx}}\ ; \quad D_y = \int_{\text{thickness}} \frac{E_y z^2 dz}{1-\nu_{xy}\nu_{yx}}\ ; \quad D_{xy} = \int G_{xy} z^2 dz$$

For an isotropic metal plate with Young's modulus E_m, Poisson's ratio ν_m and thickness t_m it follows that $D_x = D_y = E_m t_m^3/12(1-\nu_m^2)$ while $D_{xy} = D_x(1-\nu)/2$ and the critical load density is given by

$$p_x = \frac{4\pi^2}{b^2}\frac{E_m t_m^3}{12(1-\nu_m^2)} \quad (2)$$

By equalizing (1) and (2) the thickness t_h of the hybrid laminate necessary to produce the same buckling strength as a metal plate of thickness t_m can be computed. When the specific gravities of the considered plates (ρ_h and ρ_m) are known, the weight ratio of the hybrid and metal plate (W_h/W_m) can be determined from

$$\frac{W_h}{W_m} = \frac{\rho_h t_h}{\rho_m t_m} \qquad (3)$$

Above described weight ratio analysis has been carried out for hybrid-laminated plates with unidirectional-HTS ca/ep material between Al-alloy faces with different volume percentages of composite material and using 7075-T6 Al-alloy plates as reference. The calculated weight ratio curve was then verified by a test program. The results, presented in figure 1, show a good agreement between theory and experiment.

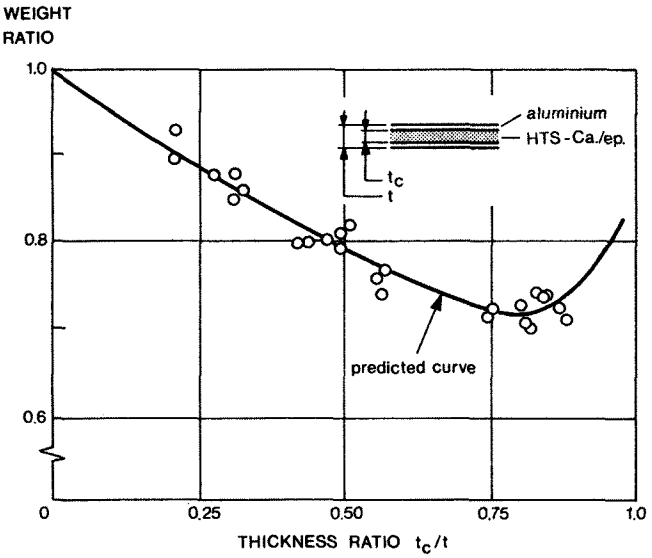

Figure 1
Weight ratio of simply supported hybrid laminates and solid 7075-T6 plates of equal width and buckling strength

A maximum weight saving of about 30 % is obtained at a composite core content of about 80 %. The weight ratio results on basis of equal ultimate buckling strength are given in figure 2.

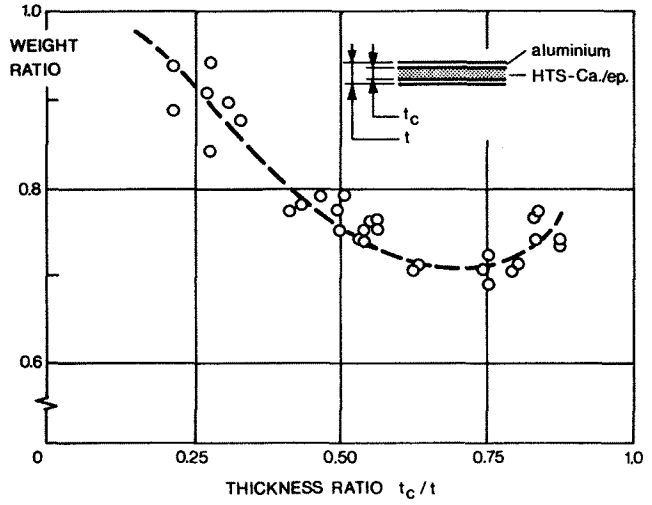

Figure 2
Weight ratio of simply supported hybrid laminates and solid 7075-T6 plates at equal width and ultimate strength

They show similar weight savings as obtained on basis of equal critical strength.

The laminates were also tested at + 60°C and - 50°C, resulting in maximum possible weight savings of 27 % and 35 %, respectively, due to the changed properties of the epoxy resin matrix. Finally, it should be noted that the buckling stresses of Al-alloy plates of high stability (low b/t_m-ratios) can be reduced considerably due to effects of plasticity. When such plates are replaced by hybrid-laminated plates, the weight savings will be even greater than represented by the graphs in figures 1 and 2.

Composite materials offer the possibility to adapt the cross sectional thickness to the local load. This implies that e.g. a composite wing-cover can be fully optimized by a gradual increase of the skin and stringers thicknesses from the tip to the root. It is interesting to know which thickness range of solid Al-alloy plates can be replaced, at equal buckling strength, by hybrid laminated plates of which the thickness is only varied by changing the composite core thickness and keeping the thickness of the metal faces constant. The results of this analysis are shown by the graph in figure 3 for laminates with a unidirectional ca/ep core and Al-alloy faces.

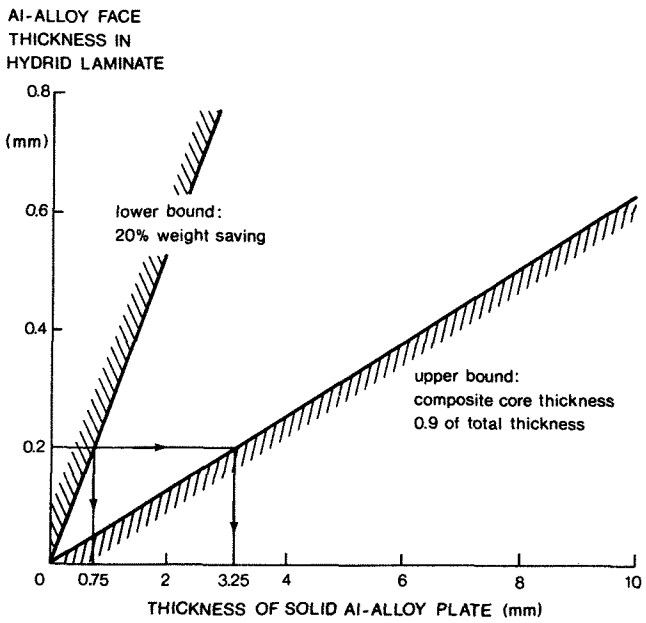

Figure 3
Thickness range of solid Al-alloy plates that can be efficiently replaced by hybrid laminates

A minimum weight saving of 20 % has been selected for setting the lower boundary and an upper boundary has been set by limiting the composite core content in the laminated plates at 90 %. It appears from this graph that, for example, a solid Al-alloy thickness range from 0.75 to 3.25 mm can be replaced, at equal critical buckling strength and plate width, by hybrid-laminates with a constant face thickness of 0.2 mm but an increasing composite core thickness.

2.2.2 Short column sections

The program of compression tests on short column sections is aimed at the development of a method to calculate the ultimate buckling strength of hybrid laminated structures.

The ∿∿-shaped sections used consist of Al-alloy faces and a uni-directional HTS-ca/ep core. A total of 16 different configurations of 3 specimens each were tested. The main variables are:

- Al-alloy face thickness: 0.3 and 0.4 mm 7075-T6
- composite core content in total cross section: 40 and 70 % by volume
- width/thickness ratio of section elements: varied between 19 and 41

A number of tested specimens is shown in figure 4:

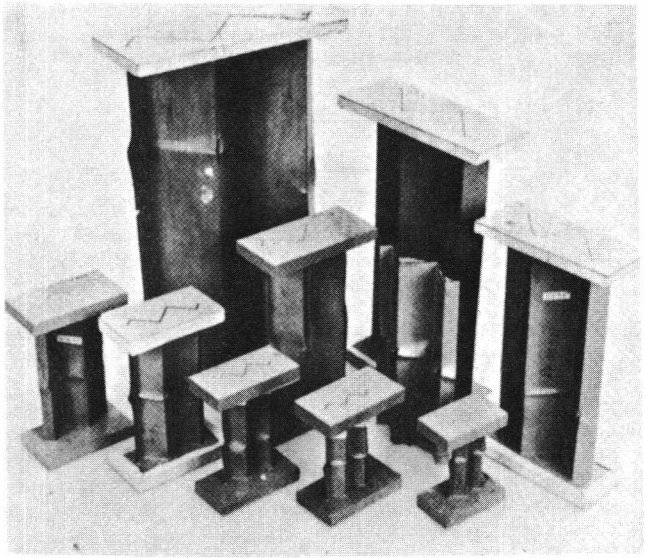

Figure 4
Hybrid laminate short column specimens after tests

The ultimate loads varied from 32 to 250 kN and the failing stresses ranged from 220 to 500 MN/m^2.

At the moment only the results of a first, rough analysis are available from which the following provisional conclusions can be made:

- the apparent critical buckling stresses are about 10 to 20 % lower than the theoretical values of simple, flat plates. This loss in performance, also observed in isotropic sheet metal structures, is probably caused by imperfections of the section elements which were considerably more serious than those present in small single flat plates.

- the obtainable weight savings compared with 7075-T6 sections of equal overall dimensions and buckling strength, seem to increase with increasing critical buckling stress of the hybrid-laminated sections as shown by the weight ratio curves in figure 5. This is explained from the higher specific compressive strength and the elastic behaviour up to ultimate compressive strength of the hybrid laminates. The buckling stresses of solid sheet metal structures of high local stability can be greatly reduced by plasticity effects.

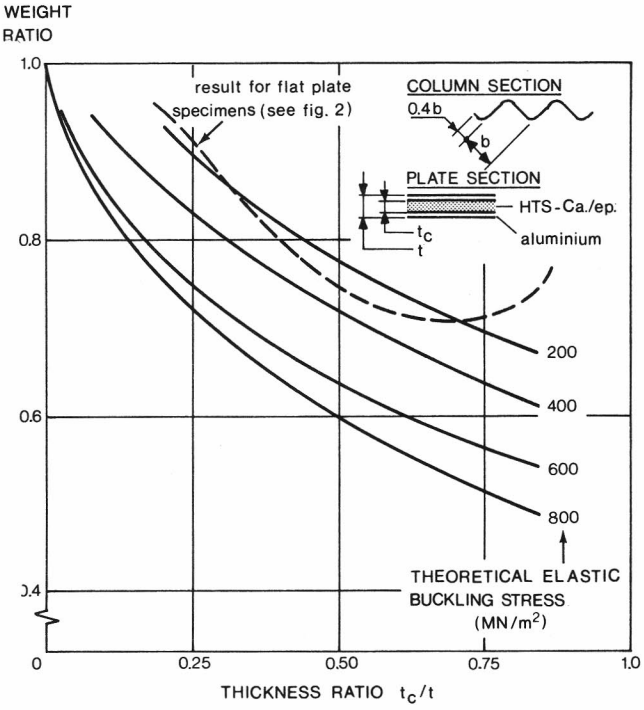

Figure 5
Weight ratio of hybrid laminate and 7075-T6 short column specimens of equal width and ultimate strength

2.2.3 Stiffened panels

A series of hat stiffened panels, made entirely of hybrid laminates, was designed, produced and tested to evaluate the producability of folded hat sections as well as assembly and testing procedures. All panels were 1200 mm long and consisted of hybrid laminate elements with .1 mm 5052 H 38 aluminium alloy face sheets. The carbon-epoxy composite core construction was different in different panels as is indicated in table 1. A general view of a test panel is given in figure 6.

TABLE 1 General data of hat-stiffened compression panels

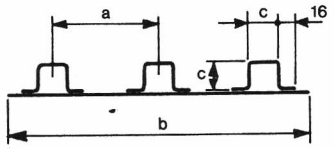

Panel type	No. of stiffeners	Dimensions (mm) a	b	c	Stiffener thickness
A	5	110	527	25	.50 ')
B	5	125	597	25	.75
C	5	125	597	25	.75
D	3	190	500	20	.25
E	5	107	516	20	.50
F	5	110	509	20	.50

') thickness of unidirectional composite core layer. All face sheets contained a .4mm $\pm 45^{\circ}$ composite core while panels C and F contained .2 and .1 mm of unidirectional layers in addition.

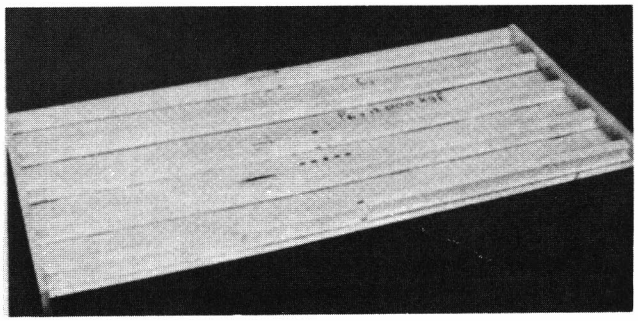

Figure 6
Hybrid laminate hat-stiffened compression test panel

During the early production stages some problems were met. It proved difficult to obtain a good adhesive bond in the vertical flanges of the stiffeners. The hybrid laminate of the stiffener was laid up on a flat table and then folded over a mandrel which also served as a curing tool (see sketch). To prevent uneven flange thickness the autoclave pressure was transferred by means of two solid triangular sections and a strip on the top flange. The assembly was cocured at 125°C under an autoclave pressure of 3 kg/cm^2 during 90 minutes. After some first products with initial curvature due to mismatch between the height of the vertical stringer flanges and of the mandrel nearly straight stiffeners were made in this fashion. Similar cocuring of the flat skin sheets presented no problems. However, cold assembly of flat sheets and slightly bent stiffeners still introduced some initial panel curvature. The skin-inward deviation per meter length is indicated in table 2.

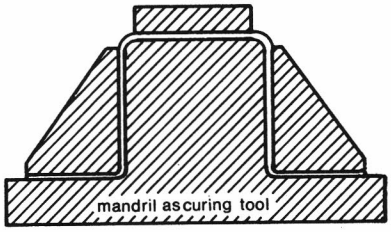

The panels were tested in a displacement controlled testing machine. The loaded ends were embedded in resin and machined flat and parallel. Further, the platens of the testing machine could be adjusted to promote a uniform strain distribution in the panel. Strain and displacement readings were taken at selected locations and initial shape and transverse displacement under load were also measured by means of a traversing displacement transducer. All panels developed skin buckles initially and final failure occurred by local stringer buckling either near the loaded end or in the middle part of the specimen depending on the sign of the initial curvature. Some raw test data are compiled in table 2.

TABLE 2 Test data of hybrid laminate hat section stiffened compression panels

Panel no.	Initial stiffener deflection δ (mm) min	max	Test load(kN) at instant of skin buckling	collapse
A1	- 0.25	0.00	30	78.1
A2	- 0.15	0.30	-	75.3
B1	- 0.10	0.15	-	118.7
B2	- 0.45	0.70	40	76.7
C1	- 0.30	- 0.10	60 - 70	117.7
C2	- 0.15	0.00	-	154.5
D1	- 0.40	0.00	-	18.-
D2	- 0.80	0.00	4	20.3

TABLE 2 (cont.

Panel no.	Initial stiffener deflection δ (mm) min	max	Test load(kN) at instant of skin buckling	collapse
E1	- 0.30	0.40	35	50
E2	- 0.55	0.15	-	54.-
F1	- 0.30	0.40	-	66.2
F2	- 0.05	0.80	30	56.4

The initial test series served the purpose of establishing production guide-lines and it provided a first insight in hybrid laminate behaviour in structural elements. The load carrying capacity of .05 to .25 MN/m is extremely low, however, and presently efforts are underway to design and manufacture panels that will carry a more realistic load level of .5 to 1.5 MN/m say.

2.3 Investigation of tensile properties

2.3.1 Static tensile properties

In a hybrid laminate the basically elastic composite material and the elastic-plastic metal are bonded together at a consolidation temperature well beyond normal operating temperatures. Then, due to differential thermal straining a state of prestress exists in the unloaded laminate at operating temperatures. Generally, the metal layers are pre-stressed in tension and under increasing tensile load the yield point is reached at a lower value of the mechanical strain than would be achieved in a solid metal plate. Upon yielding of the metal layers the tangent modulus as determined by the rule of mixtures drops accordingly. Some typical test data are shown in figure 7.

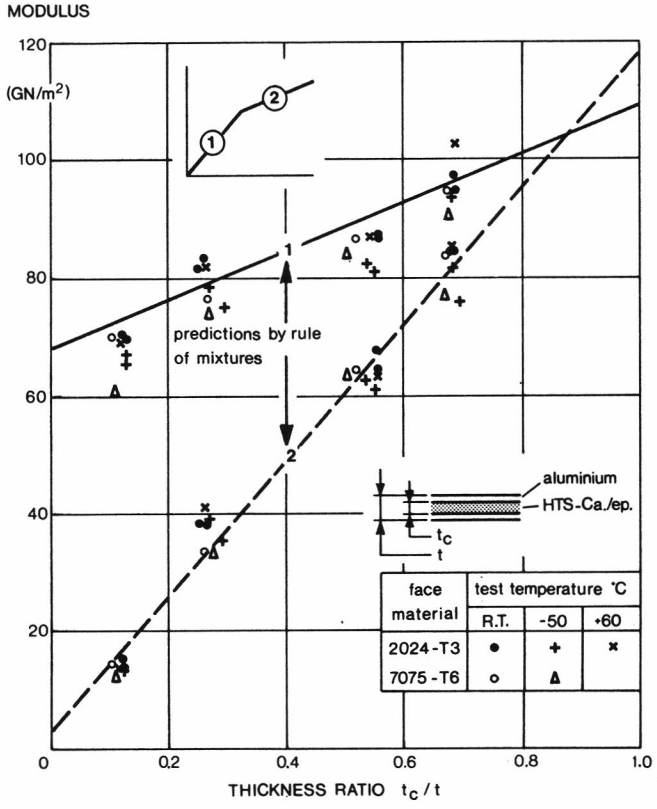

Figure 7
Measured and predicted values of primary and secondary tangent moduli of hybrid laminate

The initial tensile pre-stress in the metal is temperature dependent and so, of course, is the yield stress as is shown in figure 8.

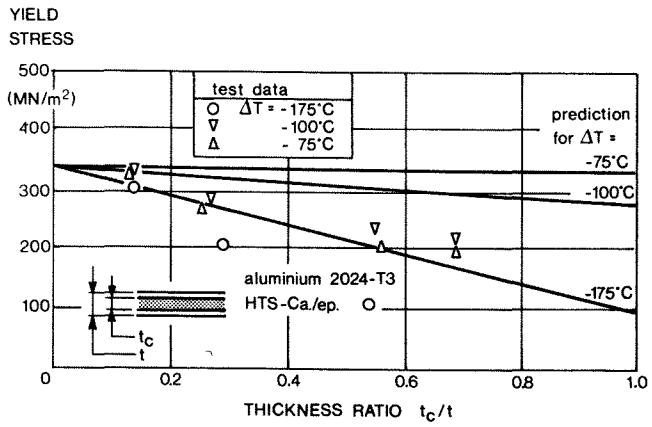

Figure 8
Hybrid laminate yield stress as a function of thickness ratio and difference, ΔT, between test temperature and consolidating temperature

A similar effect on ultimate stress is much less pronounced as is evidenced in figure 9.

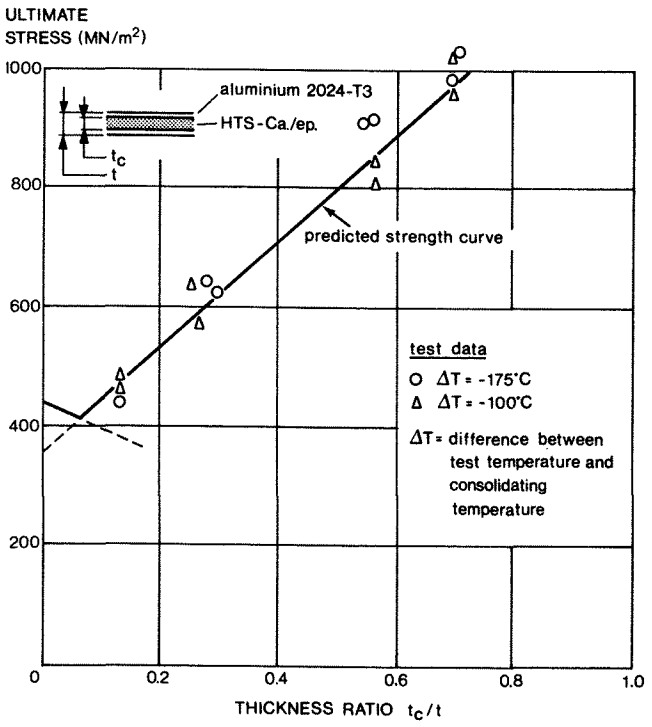

Figure 9
Hybrid laminate ultimate stress as a function of thickness ratio

The reason is that final tensile failure is governed by the allowable strain in the composite material which in case of carbon-epoxy is in the order of 1 percent. Due to initial thermal compressive strain the strain increment due to mechanical loading is larger than one percent and hence the metal will be strained well into the plastic region and the initial thermal strain effects are practically annihilated.

2.3.2 Tensile fatigue properties

The state of prestress mentioned earlier will have a profound influence on fatigue properties. The generally good fatigue resistance of unidirectional fibre composite material is partly off-set by the thermal prestress in the metal layers. Some constant amplitude testing has been done to construct endurance curves for hybrid laminates. In figure 10 room temperature test results are shown for a hot-bonded 2024-T3/ca ep laminate with a core-to-metal thickness ratio of .57.

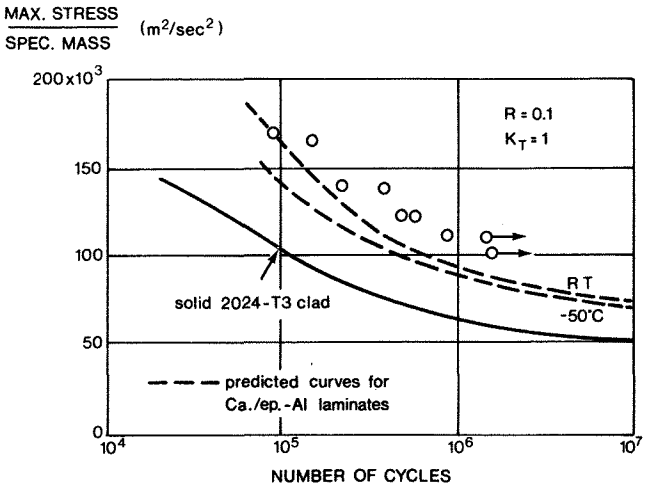

Figure 10
Constant amplitude fatigue data for hybrid laminate ($t_c/t = 0.57$)

Predictions of the endurance were made on the basis of constant amplitude data for the aluminium alloy taking account of thermal prestress. The specimens developed fatigue cracks in the metal layers only and, on the basis of a specific stress comparison the hybrid material appear to have a 50 % higher specific fatigue strength than 2024-T3. It is noted that the elastic modulus of the tested specimens which was measured at regular intervals during the fatigue test, did not show any significant change. The tests were continued in most cases up to complete failure of the metal layers.

Further constant amplitude and flight simulation fatigue testing on centre notched hybrid laminates is underway.

3. SELECTIVE REINFORCEMENT

3.1 General considerations

The excellent strength and stiffness of carbon fibres can be used most effectively to improve the quality of conventional metal aircraft structure by selective reinforcement. Several applications are known today. Although the cost-effectiveness of this form of composite application is still being questioned the more advanced concept of large scale all-composite application in primary structures seems to be a decade away still.

Selective reinforcement implies a calculated benefit in a proven conventional structure without introducing an undue amount of uncertainties and design risks. In some cases composite reinforcement was used simply to solve an ad-hoc stiffness or strength problem but in a more general sense selective reinforcement can be considered a promising structural concept in itself.

A typical one-dimensional state of loading exists in long prismatic stiffening elements of wing and fuselage panels and this situation appears to lend itself to selective reinforcement. Whereas under compressive load the stiffener has to resist both general panel instability and local buckling and transverse bending of stiffener flanges, the stringers in tensile loaded areas are essential in controlling fatigue crack growth in the sheet and in the latter case the principal loading is tensile and unidirectional.

It is recognized that a hot-bonded combination of carbon-epoxy and metal elements develops initial tensile stresses in the metal parts due to thermal incompatibility and equally undesirable compressive loading of the composite parts. The positive prestress tends to accelerate fatigue crack growth in the metal parts and, presumably, it precipitates initiation also. The high specific stiffness and strength, however, very effectively reduce the crack growth rate when the tip approaches a stiffener and in general, crack arrest capability and residual strength should be improved considerably.

Some results of a parametric study of fail-safe aspects of composite reinforced panels and of an experimental investigation of fail-safe properties of composite reinforced sandwich panels are discussed in the following paragraphs.

3.2 Parametric evaluation of fail-safe characteristics

3.2.1 Panel configuration

In the evaluation study a simple rectangular panel is considered with a length to width ratio of two. The panel is loaded in the long direction and it is provided,on both sides, with metal or composite strips or with a combination of both. The degree of stiffening is indicated by a stiffening parameter, ρ, which simply expresses the ratio of longitudinal stiffness of reinforcement and sheet. Values of the stiffening ratio varying from .50 to 1.25, representing the range of practical interest, were considered. Panel configurations containing 5, 7 or 9 stiffeners were studied.

The evaluation concentrated on two important aspects of the fail-safe philosophy that can be treated in a quantitative fashion with some degree of reliability namely, the crack propagation rate and the residual strength. The damage assumed to be present initially consists of a central crack in the sheet only or in combination with a broken central stiffener. Note that, because only an odd number of stiffeners is considered, a central crack always coincides with a stiffener location.

3.2.2 Crack rate

Predictions of crack propagation rates and crack lives are usually based on data derived from constant amplitude tests performed on simple specimens for different stress amplitude and stress ratio values. Under an arbitrary cyclic load history, however, crack growth shows accelerations and decelerations that cannot be explained from constant amplitude data. Attempts to account for these sequence effects have only been moderately successful sofar and for the present comparative study these effects will be ignored. Under this simplification the crack growth rate is estimated for a standardized fatigue load spectrum for the evaluation and testing of transport aircraft wing structures.[1] The spectrum consists of ten different stress pairs, $\overline{\sigma}_i$ and $\underline{\sigma}_i$, with equal mean stress and a relative frequency of occurrence n_i where $\sum n_i = 1$ as shown in table 3.

TABLE 3 Standardized fatigue load spectra used in crack life evaluation

Stress amplitude mean stress	Relative frequency of occurrence, n_i
1.600	.000002508
1.500	.000005017
1.300	.000012542
1.150	.000045151
.995	.000130435
.840	.000381272
.685	.002006697
.530	.010459910
.375	.087291335
.222	.899665132
	n_i = .999999999

If the crack rate for stress cycling between a maximum value $\overline{\sigma}_i$ and a minimum value $\underline{\sigma}_i$ can be formally written as

$$(da/dn)_i = f_i(\overline{\sigma}_i, \underline{\sigma}_i, a, c)$$

where a is the semi-crack length and c is a stress intensity reduction factor accounting for stiffening of the sheet then, as suggested by Schijve, the growth rate under spectrum loading can be approximated to by a weighted mixture of the form [2]

$$da/dn = \sum n_i f_i$$

The comparative crack life predictions have been derived on the basis of this simplified approach using a crack rate expression, proposed by Foreman, of the form [3]

$$da/dn = \alpha \Delta K^{\beta} / \left[(1-R)K^{*} - \Delta K\right]$$

where $\Delta K = (\overline{\sigma}_i - \underline{\sigma}_i)\sqrt{\pi a}$ and $R = \underline{\sigma}_i/\overline{\sigma}_i$. K^{*} is the plane stress fracture toughness value of the material and data for α and β should be taken from constant amplitude tests on the material under consideration. Stress intensity reduction data (c-values) were derived from energy release computations using a finite element model. For a set of parameter values, typical of aluminium alloy lower wing skin sheet material stiffened by either the same material or unidirectional HTS ca/ep or by a combination of both the life is estimated of cracks with an initial length of 10 mm and a final length equal to two stiffeners spacings. The results are given in table 4 in blocks of 4000 flights and are of relative rather than absolute nature.

It is seen from this table that due to thermal prestress in the cases considered here (mean stress of 70 MN/m^2) the crack life in a panel with all-composite stiffeners is roughly only half the life in an all metal panel.

The table also shows a shorter crack life in panels with more and consequently more closely spaced stiffeners. This may seem logical due to the fact that the final crack length is smaller in this case.

TABLE 4 Crack lives (blocks of 4000 flights) in stiffened panels

Stiffening ratio, ρ composite	metal	Sheet pre-stress MN/m^2	Number of stiffeners on panel 5	7	9
.00	.75	-	51.6	44.9	37.1
.25	.50	24	39.8	34.6	28.6
.50	.25	48	32.1	27.8	23.1
.75	.00	72	26.6	23.1	19.3
.00	1.-	-	56.1	48.9	43.4
.25	.75	21	44.6	38.8	34.6
.50	.50	42	36.6	32.1	28,6
.75	.25	63	31.1	27.1	24.1
1.-	.00	84	26.6	23.3	20.8
.00	1.25	-	59.4	52.9	45.9
.25	1.-	19	48.4	43.1	37.3
.50	.75	37	40.6	36.1	31.3
.75	.50	56	34.6	31.1	26.8
1.-	.25	75	30.3	27.1	23.3
1.25	.00	93	26.6	23.8	20.6

However, as can be seen from figure 11 the crack rate is consistently higher in the panels with more and, of consequence, lighter stiffeners.

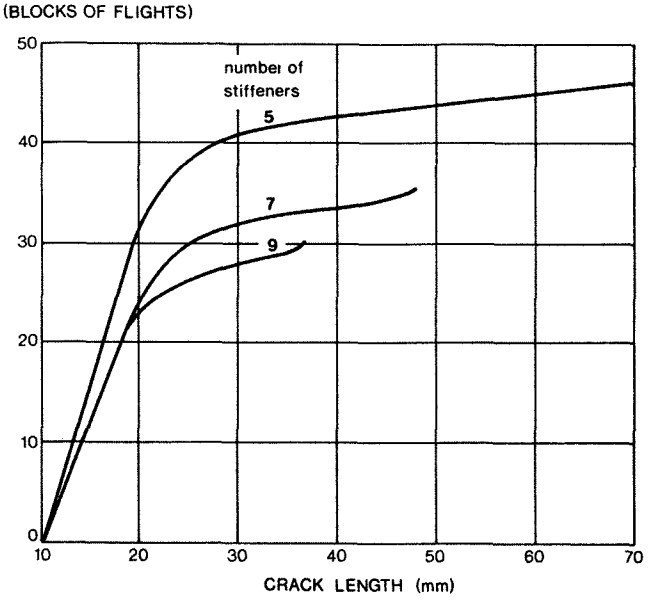

Figure 11
Crack life in panel with stiffening ratio value of $\rho = 0.50$ for different number of stiffeners (no prestress)

Similar estimates of crack life were made for the case of a central skin crack of 10 mm length in combination with a broken central stiffener again for a mean stress level of 70 MN/mm^2. In all panel configurations but one there was a chance of unstable crack growth at the initial length of 10 mm already. Either one or more or possibly even all stress amplitudes would give rise to a stress intensity exceeding the fracture toughness of the sheet material. The composite reinforced panels are considerably more sensitive due to thermal pre-stress.

3.2.3 Residual strength

Failure of a damaged stiffened panel can result from any of the following three mechanisms:
i) unstable crack growth in the sheet material that is not arrested by stiffeners.
ii) stiffener failure due to overload as a result of sheet cracks.
iii) adhesive bond failure.

Failure of the bonded connection between sheet and stiffener should not be a critical factor although relatively little is known about the sensitivity of bond strength to crack life imperfections. By a proper selection of the adhesive system and bond width bond failure should be eliminated as a primary cause of panel failure.

Stiffener failure will occur when the extra load taken by the stiffener from the sheet in the crack region exceeds the margin of strength. The magnitude of the extra load depends on stiffening ratio and crack size and is again computed by a finite element technique both for the case of an intact and of a broken central stiffener.

Finally, sheet failure is assumed to occur when the crack tip stress intensity exceeds the fracture toughness of the sheet material. The tip stress intensity is reduced by intact stiffeners across or ahead of the crack but it is raised significantly by a broken central stiffener.

In table 5 results are shown for a combination of an aluminium alloy and HTS ca/ep. Listed are the ratio of residual strength and undamaged panel strength, ζ, and an efficiency parameter η (residual strength/panel weight). Again the data should be used for comparative purposes rather than as design values, of course.

TABLE 5 Residual strength and efficiency of stiffened panels with central sheet crack

Stiffening ratios, ρ composite	metal	Strength ratio, ζ [1] ns=5	7	9	Panel efficiency, η [2] ns=5	7	9
.75	.00	.51	.50	.50	.162	.161	.159
.50	.25	.49	.49	.48	.131	.131	.129
.25	.50	.47	.47	.46	.107	.107	.106
.00	.75	.45	.45	.44	.088	.088	.087
1.00	.00	.57	.57	.56	.200	.200	.197
.75	.25	.56	.56	.55	.166	.166	.164
.50	.50	.54	.54	.54	.140	.140	.138
.25	.75	.53	.53	.52	.119	.119	.117
.00	1.-	.52	.52	.51	.101	.101	.100
1.25	.00	.62	.62	.61	.235	.235	.232
1.00	.25	.61	.61	.60	.199	.199	.197
.75	.50	.60	.60	.60	.171	.171	.169
.50	.75	.59	.59	.59	.148	.148	.146
.25	1.-	.58	.58	.58	.128	.128	.127
.00	1.25	.57	.57	.56	.112	.112	.111

1) ζ = residual strength/strength of undamaged panel

2) η = residual strength/panel weight

3) ns = number of stiffeners

It is seen that for a given stiffening ratio value the panel strength is higher for all-composite stiffeners than for all-metal stiffener by a margin of about 30 percent. The reason obviously is the higher specific strength and stiffness of the composite material as in all cases the central stiffener is the critical element. In terms of weight efficiency the panels with all-composite stiffeners show an improvement over all-metal panels roughly by a factor of two. Further it appears that for a given stiffening ratio in the cases considered here the panels with five, seven or nine stiffeners show almost identical strength and efficiency data.

Results for the case of a broken central stiffener and similar panel material as before are compiled in table 6.

TABLE 6 Residual strength and efficiency of stiffened panels with central sheet crack and broken central stiffener

Stiffening ratios, ρ		Strength ratio[1]			Panel efficiency[2]		
composite	metal	ns=5[3]	7	9	ns=5	7	9
.75	.00	.61	.66	.68	.194	.211	.218
.50	.25	.59	.65	.67	.160	.173	.179
.25	.50	.57	.62	.65	.131	.143	.148
.00	.75	.55	.60	.62	.107	.117	.122
1.-	.00	.63	.67	.69	.219	.236	.242
.75	.25	.61	.66	.68	.182	.196	.203
.50	.50	.60	.64	.66	.153	.165	.170
.25	.75	.58	.62	.64	.129	.139	.144
.00	1.-	.55	.60	.62	.109	.118	.122
1.25	.00	.64	.68	.70	.242	.256	.266
1.00	.25	.63	.67	.69	.205	.217	.225
.75	.50	.62	.65	.68	.174	.185	.192
.50	.75	.60	.64	.66	.149	.158	.165
.25	1.-	.58	.62	.64	.128	.137	.142
.00	1.25	.56	.60	.62	.110	.117	.122

1) = residual strength/strength of undamaged panel

2) = residual strength/panel weight

3) ns= number of stiffeners

Again, the all-composite stiffened panels are stronger and more efficient than all-metal panels by about the same margin as before. The failure mechanism is different now, however. First the sheet crack runs unstable across the two stiffener bays up to the next stiffener. There, crack growth is stopped and only when the off-central stiffeners fail the ultimate load is reached. Thus, the residual strength is determined largely by stiffener characteristics. When more stiffeners are applied the residual strength increases.

From the foregoing evaluation it is seen that unidirectional composite reinforcement of stiffeners in metal panels greatly increases the efficiency with regard to residual static strength. When the stiffener is the critical element in a damaged panel an all-composite stiffener may double the weight efficiency of the panel.

Also, in case of extreme thermal incompatibility of metal and composite, the positive pre-stress in the metal sheet accelerates crack growth. Typically in a panel with aluminium alloy sheet and HST ca/ep stiffeners the crack rate in the sheet may be doubled as compared to an all-metal panel.

For panels with a two-bay skin crack and a broken stiffener the residual strength increases somewhat when lighter but more closely spaced stiffeners are applied.

3.3 Reinforced sandwich panel tests

The concept of composite reinforcement to improve fail-safe characteristics was applied in a series of aluminium alloy sandwich panels. The panels, as shown in figure 12, consisted of 1 mm clad 7075-T6 faces and a 30 mm thick core layer of 5056 aluminium foil honeycomb.

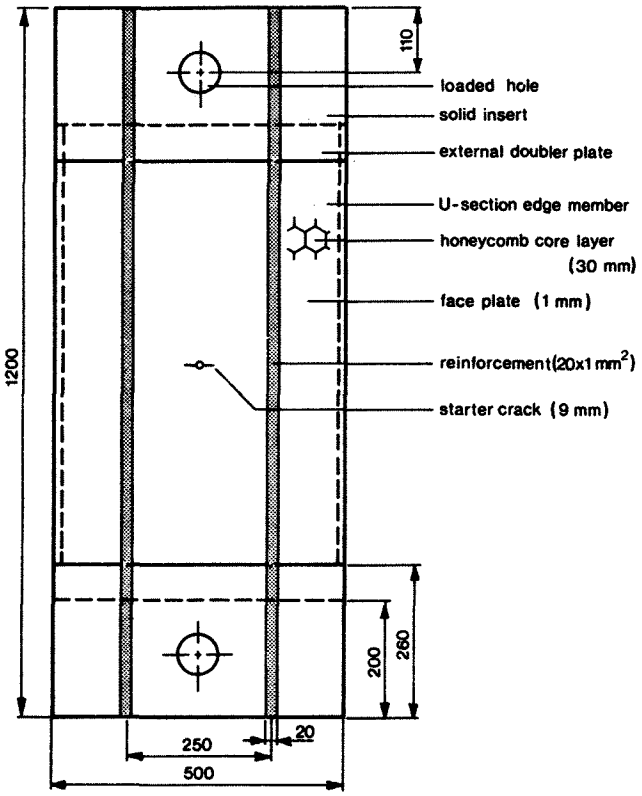

Figure 12
Principle dimensions and construction of test panels

Two 20 x 1 mm^2 reinforcing strips of uniaxial HTS ca/ep material were bonded onto each face layer and a central saw cut in one of the face layers acted as a starter notch. The panels were provided with very stiff solid inserts at the loaded ends to promote a uniform strain distribution away from the cracked region. The unloaded ends contained U-formed sections added to protect the core layer.

The panels were fatigue-loaded to grow a sharp notch of predetermined length in one of the faces after which the residual strength was determined in a static tensile testing machine. In figure 13 the more important test data are shown together with residual strength data of similar panels without composite reinforcement.

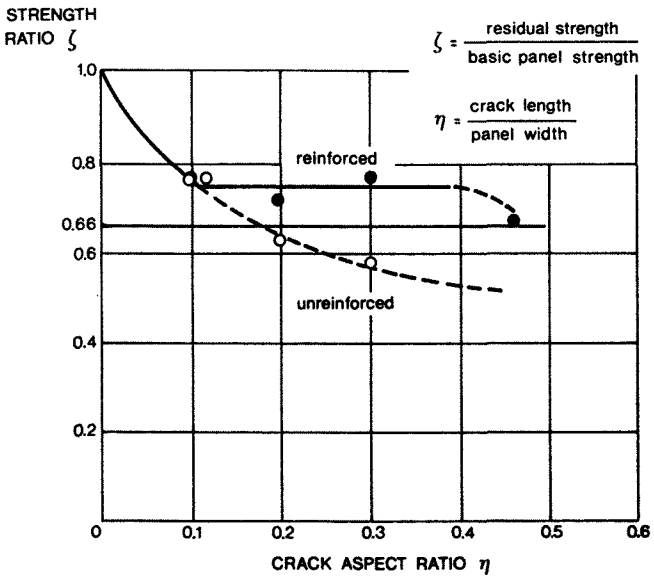

Figure 13

Residual strength diagram; residual strength of reinforced and unreinforced panels compared to the same basic strength figure viz. the ultimate strength of an undamaged, unreinforced panel

It is seen that except for very short crack lengths, where initial crack instability leads to total panel failure, the reinforced panels are stronger than the unreinforced in the same manner as stiffened panels differ from unstiffened sheets: cracks that become unstable at a given panel load may be arrested by a stiffening element. In the present test series temporarily unstable growth did occur for short cracks while the longer cracks extended in a stable fashion up to the composite strips. Final panel failure appeared to be governed entirely by failure of the composite reinforcements. As indicated in the figure a strength of two thirds of the undamaged panel strength was maintained in all specimens due to a reinforcement that added only three percent to the panel weight.

4. REFERENCES

1. de Jonge, J.B., Schütz, D., Lowack, H. and Schijve, J. — A standardized load sequence for flight simulation tests on transport aircraft wing structures. NLR TR 73029 U (also LBF-Bericht FB-106), March 1973.

2. Schijve, J. — The accumulation of fatigue damage in aircraft materials and structures. AGARDograph no.157, January 1972.

3. Forman, R.G., Kearney, V.E. and Engle, R.M. — "Numerical analysis of crack propagation in cyclically loaded structures". Journal of Basic Engineering, Trans.ASME, 1967, 89, p.459.